Application of an offshore wind farm layout optimization methodology at Middelgrunden wind farm

Citation for published version:
Pillai, A, Chick, J, Khorasanchi, M, Barbouchi, S & Johanning, L 2017, 'Application of an offshore wind farm layout optimization methodology at Middelgrunden wind farm' Ocean Engineering. DOI: 10.1016/j.oceaneng.2017.04.049

Digital Object Identifier (DOI):
10.1016/j.oceaneng.2017.04.049

Link:
Link to publication record in Edinburgh Research Explorer

Document Version:
Peer reviewed version

Published In:
Ocean Engineering

Application of an offshore wind farm layout optimization methodology at Middelgrunden wind farm

Ajit C Pillai[a,b,c], John Chick[a,d], Mahdi Khorasanchi[a,e], Sami Barbouchi[b], Lars Johanning[a,c]

[a] *Industrial Doctorate Centre for Offshore Renewable Energy, The University of Edinburgh, Edinburgh, UK*
[b] *EDF Energy R&D UK Centre, London, UK*
[c] *College of Engineering, Mathematics, and Physical Sciences, University of Exeter, Penryn, UK*
[d] *Institute for Energy Systems, The University of Edinburgh, Edinburgh, UK*
[e] *Department of Naval Architecture, Ocean, and Marine Engineering, University of Strathclyde, Glasgow, UK*

Abstract

This article explores the application of a wind farm layout evaluation function and layout optimization framework to Middelgrunden wind farm in Denmark. This framework has been built considering the interests of wind farm developers in order to aid in the planning of future offshore wind farms using the UK Round 3 wind farms as a point of reference to calibrate the model. The present work applies the developed evaluation tool to estimate the cost, energy production, and the levelized cost of energy for the existing as-built layout at Middelgrunden wind farm; comparing these against the cost and energy production reported by the wind farm operator. From here, new layouts have then been designed using either a genetic algorithm or a particle swarm optimizer. This study has found that both optimization algorithms are capable of identifying layouts with reduced levelized cost of energy compared to the existing layout while still considering the specific conditions and constraints at this site and those typical of future projects. Reductions in levelized cost of energy such as this can result in significant savings over the lifetime of the project thereby highlighting the need for including new advanced methods to wind farm layout design.

Keywords: offshore wind farm layout optimization, levelized cost of energy, genetic algorithm, particle swarm, Middelgrunden wind farm

1. Introduction

As offshore wind farms continue to grow it has become increasingly important to ensure that these projects are managed as efficiently as possible. With this in mind, the field of offshore wind farm layout optimization has grown to include sophisticated methodologies for the evaluation of the levelized cost of energy (LCOE) of offshore wind farms which includes both the lifetime energy production and lifetime costs of the wind farm. The LCOE, is frequently used by project developers to evaluate the impact a change in design might have on a project. This metric is also preferred as it is technology agnostic and therefore gives a basis by which projects of different technology types can easily be compared against one another.

The present work expands on the standard paradigm for the optimization of offshore wind farm layouts in which wake and cost models are integrated as the evaluation function for an optimization algorithm. This work shows that a sophisticated and detailed LCOE evaluation tool can successfully be included in the optimization process accounting for realistic constraints faced by a wind farm developer. Taking the UK Round 3 wind farms as a point of reference, the present tool built in partnership with wind farm developers, has been developed to aid in the planning of these wind farms allowing the developer to explore wind farm layout alternatives. Given the future application to UK Round 3 sites, much of the tool has been calibrated to these sites and sites of similar site characteristics. Extending the previous work of the authors [1], the present work allows the wind farm to be designed considering different degrees of layout restriction which may potentially be imposed by regulatory bodies.

This article explores Middelgrunden wind farm, a wind farm off the Danish coast, as a test case to both verify the full LCOE evaluation function and highlight potential improvements that could have been achieved through more optimal turbine placement using either a genetic algorithm (GA) or a particle swarm optimizer (PSO). By applying the layout optimization framework to a real wind farm site rather than to fictional cases the capabilities and applicability of the present wind farm layout optimization tool are demonstrated.

The field of wind farm layout optimization was initially explored in the seminal work by Mosetti et al. [2] in which three fictional wind farm sites were defined and wind farms optimized using a genetic algorithm. Following the inception of the field of optimization of wind farm layouts, the cases defined by Mosetti et al. [2] have been revisited and used as a benchmark. The field has explored a number of different optimization algorithms to this problem including genetic algorithms [3–12], particle swarm optimizer [13], viral based optimization [14], pattern search [15], mixed-integer linear programming [16], and Monte Carlo simulation [17]. The most frequently deployed optimization approach has been the genetic algorithm and though much work has focused on the development and evolution of the optimization algorithm, little of the existing literature has explored the evolution of the evaluation function beyond testing alternate wake models. Detailed reviews in the field of wind farm layout optimization have been compiled by Tesauro et al. [18] and Herbert-Acero et al. [19].

As the original work by Mosetti et al. [2] explored the applicability of the genetic algorithm to this problem, it ignored the layout dependent costs. Many of the developed tools following this have also focused on the applicability and development of the optimization and have therefore opted to use cost functions that either omit important layout dependent factors or which ignore the layout all together thereby only considering the impact the layout has on the energy produced. The work by Elkinton [4] represents an exception in which a detailed cost model was built and verified. This, however, was developed based on published data at the time and has limited applicability to new projects. As the aim of the existing tools has been to further develop the optimizers rather than industrial applications of the methods, it remains challenging for the developed wind farm layout optimization tools and methodologies to be deployed in the design of real offshore wind farms. Focusing more on the potential industrial applications, the present work therefore both represents a more detailed evaluation function over previous work and also applies the full methodology to a more complex wind farm site with realistic constraints faced by developers. Furthermore, the development of the present framework has allowed two of the leading metaheuristic optimization algorithms applied to offshore wind farms to be deployed on the same framework allowing a direct comparison.

Through the deployment of this tool for an existing wind farm it is possible to gauge the tool's suitability to future wind farms and identify areas in which the tool will need to be further developed in order for the results to be of use to a site developer.

2. Methodology

The developed approach makes use of a modular framework for the assessment of offshore wind farm layouts. As is shown in fig. 1, the evaluation of a layout is divided into three separate steps. The LCOE by definition requires the computation of the AEP and the lifetime costs as shown in eq. (1), however, a wind farm's electrical infrastructure (substation position, intray-array cable paths, and intra-array cable specifications) impacts both of these terms; changes in the electrical infrastructure affect the energy losses and therefore the AEP while at the same time changes in the electrical cabling and substation position can directly affect the costs. The first step in the evaluation of the LCOE is therefore for the necessary electrical infrastructure to be determined for a given turbine layout. Following this, the annual energy production (AEP) for the wind farm is computed considering not only the wake losses, but also the losses due to the electrical infrastructure; and finally, the relative costs of the project over its lifetime are estimated. From these three components, the LCOE of the layout is computed and as a result, the optimizers can use this information to make informed decisions on how the solutions should evolve between generations.

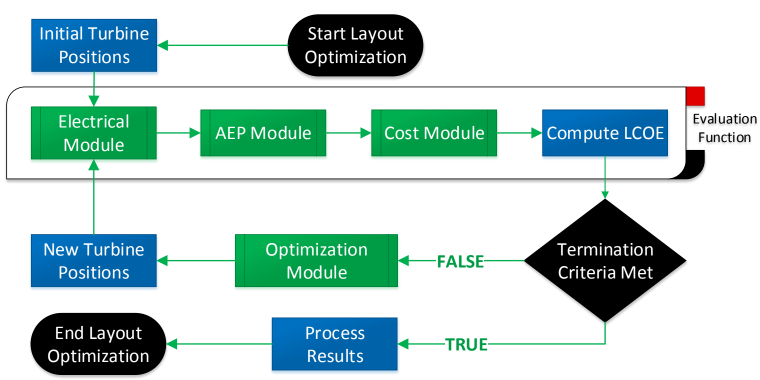

Figure 1: Modular approach to wind farm layout optimization.

The LCOE is defined to be a function of both the total energy generated and the costs over the lifetime of the wind farm:

$$LCOE = \frac{\sum_{t=1}^{n} \frac{C_t}{(1+r)^t}}{\sum_{t=1}^{n} \frac{AEP_t}{(1+r)^t}} \quad (1)$$

where C_t is the total costs incurred in year t, n is the project lifetime, AEP_t, is the annual energy production in year t, and r is the discount rate of the project.

As European regulators are currently in discussions with wind farm developers to develop guidance on how layouts are to be designed in the future, there are different levels of constraint which are of interest to developers depending on the final decisions made by the regulators and licensing bodies [20]. In order to accommodate these different levels of constraint, the present framework has three separate modes of operation which address these different constraints:

1. **Array Mode** - The decision variables define the spacing and orientation of a regular grid of turbine positions with constant downwind and crosswind spacing throughout the site. This produces layouts with clearly defined navigational channels and is preferred by some regulators due to stakeholders concerns such as those raised by the Maritime Coastguard Agency in the UK [20].
2. **Binary Mode** - The wind farm area is discretized into allowable turbine positions and the decision variables are therefore binary variables representing the presence of a turbine in a particular cell. Wind farm developers are interested in this approach as it allows them to have much of the regularity that regulators seek with the array mode, but could allow for more innovative layouts that better use the site in question. In this scenario, the discretized allowable turbine positions could be imposed directly with the regulator or be developed through discussions between the wind farm developer, regulator, and other stakeholders.
3. **Continuous Mode** - The decision variables directly define the turbine coordinates and may therefore occupy any value within the wind farm area. Using these constraints, there are no externally regulator/stakeholder imposed constraints on the positions of the turbines

and this therefore represents the case in which the wind farm developer is free to develop the site as they see best.

2.1. Electrical Infrastructure Optimization

As part of the development of this layout optimization framework, a sub-tool has been developed to address the optimization of an offshore wind farm's electrical infrastructure. This is fully presented by in Pillai et al. [21]. This sub-tool implements a heuristic approach and is therefore not guaranteed to find the proven optimal solution, however, it takes a pragmatic approach, identifying good feasible solutions in an acceptable run time. As part of this sub-tool, given the turbine positions, number of offshore substations, voltage level of the connection network, and the cable parameters, the offshore substation positions are determined as well as all intra-array cable paths, and cable sizes. In the case of Middelgrunden wind farm, there is no offshore substation and therefore this sub-tool is only used to determine the cable paths considering the voltage level and the cable specifications/limits.

Within this sub-tool, a pathfinding algorithm is executed to determine the possible cable paths which could connect the wind farm. For the present case study, the pathfinding algorithm was run between all turbine pairs allowing any turbine to potentially be connected to any of the other turbines or the onshore connection point. The pathfinding algorithm is used to ensure the consideration of seabed obstacles which define where the cables cannot be placed. Using the accurate lengths of cables determined by the pathfinding algorithm, a capacitated minimum spanning tree (CMST) problem is formulated and solved using the commercial MILP solver Gurobi [22]. The solution to the CMST identifies which of the possible cables should be deployed in the final network. In this way, the pathfinding step defines all the possible cables to consider and their accurate lengths, while the CMST selects which of these cables should be used to minimize the cost of the infrastructure.

In Pillai et al. [21] this methodology is presented in full and demonstrate that this new methodology can be necessary for large offshore wind farms which may need to consider a number of obstacle regions where either cables or substations cannot be placed. Though cable path optimization has previously been previously explored using a MILP formulation by Fagerfjäll [16]; Lindahl et al. [23]; Bauer and Lysgaard [24]; and Dutta and Overbye [25], the present methodology has greater capabilities in the handling of complex seabed constraints which are now faced by wind farm developers at future sites. Inclusion of such a detailed cable path optimization within the offshore wind farm layout optimization problem has previously not been undertaken, however, is a feature sought by wind farm developers.

2.2. Annual Energy Production

Due to the extraction of energy, wind turbines impact the air flow reducing the wind speed and increasing the turbulence directly behind an operating wind turbine [26–29]. As a result of this, the wind farm layout has a major impact on the wind speeds that each individual wind turbine within the wind farm experiences and therefore a direct impact on the energy produced by the wind farm. It is therefore important that the wind turbine wakes are accounted for.

The calculation of the AEP is done in a traditional approach which accounts for the wake losses throughout the wind farm using the analytic wake model developed by Larsen [30]. This wake model has been deployed here as validation at several existing wind farms has demonstrated that it represents a good compromise between computational speed and model accuracy when used to compute the AEP of an offshore wind farm [31, 32]. Though there are models which have been able to more accurately estimate the AEP such as those based on computational fluid dynamics, these require additional computational time rendering them less effective when deployed in the optimization process where the AEP calculation will be done for each layout considered.

To compute the AEP, each wind speed and direction combination are stepped through in sequence using $1\,\mathrm{m\,s^{-1}}$ and 30° bins. For each free wind speed and wind direction the analytic wake model is used to update each turbine's incident wind speed based on the performance of all upwind turbines. From this, the wind turbine power curve is used to convert the wake affected incident wind speed to the energy produced under these conditions [33, 34]. For each wind speed and direction combination, the electrical cable losses are then computed based on each turbine's individual contribution to the AEP using an IEC based methodology [35–37]. Following this, the total wind farm contribution to AEP under the given free-stream wind speed and direction is updated. This total production for each wind speed and direction combination is then scaled by the probability of occurrence of this combination for the site in question before being added to the AEP.

$$AEP = 8766 \times \sum_{\theta_i} \sum_{v_i} P(\theta_i, v_i) \times \left[E(\theta_i, v_i) - L\left(E(\theta_i, v_i)\right)\right] \tag{2}$$

where θ_i is the wind direction; v_i is the wind speed; $P(\theta_i, v_i)$ is the joint probability of θ_i and v_i; $E(\theta_i, v_i)$ is the energy production for the wind farm for the combination of free wind speed and direction considering the wake losses; and $L(E(\theta_i, v_i))$ is the electrical losses associated with the energy production as a result of the intra-array cable network. $E(\theta_i, v_i)$ therefore represents the gross energy measured at each turbine nacelle, while $E(\theta_i, v_i) - L(E(\theta_i, v_i))$ represents the net energy delivered to the grid.

2.2.1. Larsen Wake Model

In the computation of the AEP, this tool makes use of the Larsen wake model [30]. This wake model is an analytic wake model which models the reduction in wind speed as a result of an operating wind turbine. The model is based on a closed-form solution to the Reynolds-Averaged Navier-Stokes (RANS) equations based on Prandtl mixing theory [30, 38]. The full formulation of this model is given in Larsen [30]; Larsen [38]; and Tong et al. [39].

This model uses the wind farm layout, wind speed, wind direction, ambient turbulence intensity, and the turbine thrust curve to estimate the wind speed deficit at a desired downwind location. By iterating through the turbines starting with the most upwind turbine given the wind direction, the wind speed deficit can then be computed for each turbine in sequence thereby determining the effective wind speed observed by each turbine for the given conditions. The effect of multiple and overlapping wakes is taken into account using a root-sum-square method [31, 32].

2.3. Cost Estimation

Previous tools that have included a cost model have typically not been able to validate their cost models, and as a result have introduced significant uncertainty into the optimality of their solutions [4, 16]. As this tool has been developed in conjunction with an offshore wind farm developer, it has been possible to directly develop, calibrate, and validate the cost assessment methodologies against real industry costs. Consequently this work presents costs that have been parameterized and validated against the real costs to be incurred by large offshore wind farms deploying wind turbines in the 5-8 MW range in UK waters. Some discrepancy is therefore anticipated as in this study, the model is being applied to a much smaller offshore wind farm, utilizing smaller wind turbines, and located in Danish waters.

From discussions with wind farm developers and component suppliers, the total cost of the wind farm is divided into eight major cost elements each with varying degrees of sensitivity to the layout qualitatively described in table 1 based on how the layout is considered in the calculation of each individual cost element. Each cost element is attributed to being part of the capital expenditure (CAPEX) incurred during the construction period of the wind farm, the operational expenditure (OPEX) incurred annually during the operational period of the wind farm, or the decommissioning expenditure (DECEX) incurred during the decommissioning period at the end of project life. For each of the cost elements, industry standard assumptions for vessel parameters have been assumed.

Table 1: Cost Element Contribution to CAPEX, DECEX, and OPEX

Cost Element	CAPEX	DECEX	OPEX	Sensitivity to Layout
Turbine Supply	✓	-	-	Low
Turbine Installation	✓	-	-	Medium
Foundation Supply	✓	-	-	Medium
Foundation Installation	✓	-	-	Medium
Intra-Array Cables	✓	-	-	High
Decommissioning	-	✓	-	Medium
Operations and Maintenance	-	-	✓	Medium
Offshore Transmission Assets	✓	-	✓	Low

2.3.1. Turbine supply

The turbine supply costs are determined based on the price per turbine including tower that turbine manufacturers have provided through discussions with various members of the offshore wind industry. This cost therefore does not vary due to the layout unless the total number of turbines or installed capacity changes.

2.3.2. Turbine installation

Each of the installation stages takes a time based approach in which the time required for the installation operations is computed and then computed to a cost based on the vessel and crew day rates [40, 41]. The turbine installation costs are based on market values for vessel costs and capacities. These costs are modeled by first calculating the expected time required to install all the turbines at their specific locations. This includes not only the computation of the travel time between the turbines, but also the necessary time to go to and from the construction port. To calculate this, the turbines are clustered based on the capacity of the installation vessel, and for each cluster a shortest path is computed between the port, each turbine in the cluster, and the port again using Dijkstra's algorithm. This approach therefore accurately computes the distance that the vessel must traverse during the installation process. From this, the total time is computed based on assumed weather availability and time required for each operation once at the turbine positions. The costs are then computed based on the vessel and equipment day rates. The turbine layout, therefore, has a direct impact on the time needed to travel between turbine positions as well as to and from the port. This cost model differs from common approaches through the use of the clustering and pathfinding algorithms used to determine the distance that the vessel must cover in the installation procedure. This is a necessary element to characterize the impact that the wind farm layout has on the costs.

2.3.3. Foundation supply

The foundation supply costs include the cost of the transition piece and delivery of a fabricated foundation to the installation port. Foundation costs are found to be highly dependent on the site conditions where the foundation is to be installed. To account for this dependence, previous cost models have attempted a bottom up approach based on the soil characteristics at the installation site to model the costs. Unfortunately this approach has proven difficult to validate for all types of foundations due to the very detailed input data required [4]. Furthermore, wind farm layout optimization tools are generally deployed in early stages of the wind farm design at which point detailed soil surveys have not always been completed. In order to remain applicable to the use case of wind farm developers it was found that simpler cost models would be needed. The present tool therefore makes use of separate empirical relationships for gravity based foundations, monopiles, and jackets which have been developed from discussions with manufacturers. Specific soil conditions are not included, however, the water depth, turbine size, and turbine loads are. Detailed bathymetry of the site is therefore necessary in order to estimate the variation in gravity based foundation supply costs as a function of the turbine layout [42, 43]. As Middelgrunden wind farm has turbines installed on gravity based foundations, only this cost relationship is used in the present study.

2.3.4. Foundation installation

The foundation installation process, like the turbine installation module, is based on estimating the time required to complete the operations and converting this time to a cost. Unlike the turbine installation though, this is modeled as three distinct phases which each use a different vessel to complete.

Regardless of the foundation type (gravity-based, monopile, or jacket), some seabed preparation is necessary. For a gravity-based foundation this might be the necessary dredging and leveling of the seabed, while for monopiles and jackets this would more likely be pre-pilling works including surveying and drilling. After this step, the foundations will be installed as a separate operation following which some kind of scour protection will often be added. The installation of scour protection is again modeled as a separate step involving a different vessel from either the site preparation or foundation installation processes. The cost of the material used for scour protection is included in this step rather than the foundation supply costs. In some conditions, the scour protection will not be necessary, however, for the time being this model has assumed that all turbines will require scour protection.

2.3.5. Intra-array cable costs

The intra-array cables are decomposed into horizontal lengths which are buried and connect between turbines, and the vertical lengths which connect from the seabed to a turbine nacelle. The vertical lengths therefore include consideration of the water depth at the turbine position and the turbine hub height. The total horizontal length of the required intra-array cables is computed from the intra-array cable optimization tool described in section 2.1. This tool has the capability for optimizing the layout for different cable cross-section sizes and therefore can output not only the total length of cable, but the horizontal lengths required for each segment and the required cross-section. From this, the intra-array cable cost module computes the necessary vertical cable and the necessary spare cable before computing the costs.

The installation cost for the intra-array cables is computed in a similar manner as the turbine and foundation installation modules. This is done based on data available for cable trenching vessels and therefore assumes that all cables are trenched and buried.

2.3.6. Offshore Transmission Assets

Regulators in different countries each have different ways in which the offshore transmission assets are handled and which of these costs are incurred by the wind farm developer. In Denmark, the offshore substation (if present), the offshore export cable, and onshore works are all built and owned by the Transmission System Operator (TSO) Energinet.dk. As a result, there is no need when considering Danish projects to include these cost elements as they are not incurred by the project developer.

2.3.7. Operations and Maintenance

The operations and maintenance (O&M) costs are modeled based on the anticipated operations and maintenance costs for projects in the 500 MW to 1000 MW. These costs are then modeled as a function of both with the capacity of the wind farm and its distance to shore. As this term is impacted by distance of the wind farm to the operations and maintenance port, this too is affected by the layout. The operations and maintenance costs are classed as operational expenditure (OPEX) as these are incurred annually in each year of operation.

2.3.8. Decommissioning

The decommissioning costs include the removal of the turbines and foundations. Presently, it is unclear what will happen to the transmission and export cables at the end of life, and the model therefore assumes that these cables are not removed at the time of decommissioning, but simply cut at the turbines and substation, leaving the buried lengths as they are. The decommissioning costs are therefore modeled similar to the turbine and foundation installation processes. The time requirements for each vessel is first computed and this is then converted to a cost based on the vessel day rates [40, 41]. Like the installation processes it is assumed that the vessels have some capacity and must return to the decommissioning port prior to completion of the overall operation. The turbines and foundations are assumed to be decommissioned in separate steps requiring separate vessels. Like the installation phases, this term is therefore dependent on the turbine positions and is affected by the layout under consideration.

2.4. Optimization Algorithms

The final step of the framework is to integrate an optimization algorithm to the evaluation in order to propose new layouts which are evaluated using the LCOE function described above. For the present work, a genetic algorithm (GA) and a particle swarm optimization (PSO), two algorithms commonly used in engineering applications, have been implemented and applied to Middelgrunden. For both algorithms, the problem was addressed exploring three different levels of constraint corresponding to different constraints that regulators are considering for wind farms [20].

Given the complexity of the wind farm layout optimization evaluation function and thereby the decision problem, population based metaheuristics were thought to be well suited as these have been shown to be effective ways of exploring complex search spaces. Metaheuristics by definition identify good solutions in an acceptable time frame and do not guarantee that an optimal solution is found. For complex search spaces, however, they represent a pragmatic approach for identifying a relevant feasible solution. Though other algorithms such as gradient decent, interior-point methods, and classical techniques could be deployed for this problem, it is believed that population based algorithms would be more capable. Within the family of population based algorithms, the GA and PSO are thought of as fundamentally different types of algorithms as GAs take on a competitive approach within the population while PSOs take on a cooperative approach. Though the GA has been deployed to a range of engineering problems, usually to quite successful results, the PSO is a younger algorithm that has not seen as frequent deployment. Given that the present framework has been developed in part to allow different algorithms to be compared within the same framework, using the same problem formulation and evaluation function it was decided that these two algorithms would be explored.

2.4.1. Genetic Algorithm

The genetic algorithm represents a metaheuristic algorithm commonly deployed to aid in decision making and engineering design. In existing work, the GA has been frequently applied to wind farm layout design [19].

The GA is so named because it borrows principles from biology and evolutionary processes to generate and test new solutions. Each generation of the GA begins with *selection* through which pairs of individuals already in the population are chosen, based on the quality of their solutions, to contribute genetic material to the next generation. These pairs of individuals are combined through the *crossover* and *mutation* operators to generate new solutions referred to as child solutions. These child solutions take part of their parents' solutions through crossover, and are then potentially randomly altered during mutation. Through these two operations the GA attempts to retain the good elements of the parents in the newly generated children, and the random element is included to aid in the avoidance of local solutions. A *replace weakest first* replacement strategy is then employed to determine which of the new generated children are included in the next generation. This process of selection, crossover, and mutation repeats until an identified proportion of the population has been replaced and the overall population has improved in quality which marks the end of a generation. In general GAs continue for a predefined number of generations or until there is insufficient diversity within the population, that is until the number of unique members of the population falls bellow a threshold value. The overall flow of the GA is shown in fig. 2. Though both crossover and mutation consider the constraints, after both crossover and mutation, the constraints are explicitly imposed, and if a child solution fails to satisfy any of the constraints then crossover and mutation are repeated until it does [44, 45].

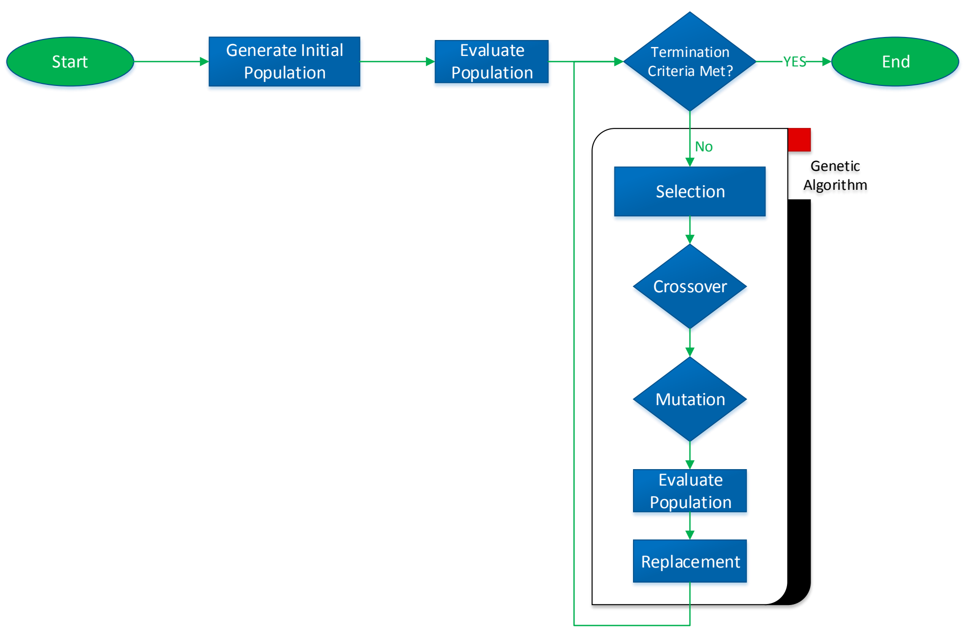

Figure 2: Genetic algorithm overview

In order to improve the convergence rates and the avoidance of local solution, the probabilities associated with crossover and mutation have been made adaptive in the implemented GA and are functions of the quality of the solution. In this way, a better solution not only has a higher probability of being selected, but also a higher probability of contributing through crossover. The crossover and mutation probabilities are therefore a function of the solution's fitness value (f) or the fitness value of the best parent (f') compared to the population's mean fitness $\left(\bar{f}\right)$ or the population's best fitness (f_{max}).

The below formulations ensure that as the population converges, as measured by the difference between the fitness of the best individual and the mean fitness value of the individuals in the population, both higher crossover and mutation rates are applied to increase the exploration parameters of the GA and avoid premature convergence. At the same time, to preserve the better solutions in the population, crossover and mutation rates are decreased for these individuals.

$$p_c = \frac{k_1 \left(f_{max} - f'\right)}{f_{max} - \bar{f}} \qquad \text{for} \qquad f' \geq \bar{f} \tag{3}$$

$$p_c = k_3 \qquad \text{for} \qquad f' < \bar{f} \tag{4}$$

$$p_m = \frac{k_2 \left(f_{max} - f\right)}{f_{max} - \bar{f}} \qquad \text{for} \qquad f \geq \bar{f} \tag{5}$$

$$p_m = k_4 \qquad \text{for} \qquad f < \bar{f} \tag{6}$$

where p_c and p_m are respectively the probability of crossover and mutation. The constants are defined such that $k_1 = k_3 = 1$ and $k_2 = k_4 = \frac{1}{2}$. The use of adaptive parameters like this has been found to both aid in the rate at which the process converges as well as its ability to avoid local solutions [46, 47].

2.4.2. Particle Swarm Optimizer

An alternate population based optimization algorithm is the particle swarm optimizer (PSO). This algorithm considers the candidate solutions as particles exploring the search space. From generation to generation, the particle's position within the search space changes depending on the quality of its current position relative to the best position the particle has historically occupied and the best historical position within the swarm at large. This process is shown in fig. 3.

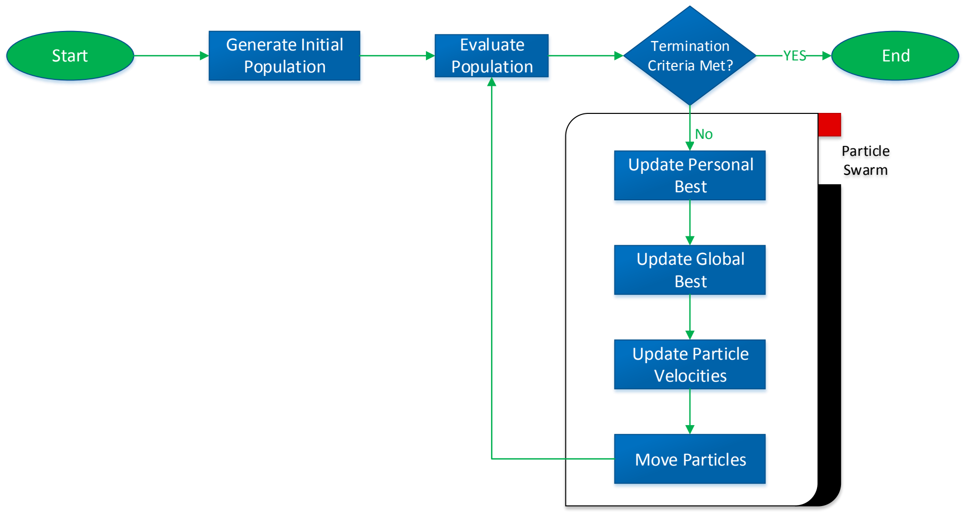

Figure 3: Particle swarm optimization overview

The particles' change in position within the search space is given each iteration by the velocity. A particle's velocity in iteration i, v_i is given by:

$$v_i = w_i v_{i-1} + C_1(p - x_{i-1}) + C_2(g - x_{i-1}) + C_3(\eta - x_{i-1}) + C_4 \times rand \quad (7)$$

where, w is an inertia weight determined by tuning the PSO; C_1, C_2, C_3, and C_4 are coefficients representing the weighting of each of the contributors determined by tuning the PSO; p is the best position that the particle has historically occupied within the search space; g is the best historical position that the swarm as a whole has ever occupied; x is the solution under consideration; η is the best historical position that the neighborhood as a whole has ever occupied; and $rand$ is random number between 0 and 1. With this velocity the particle's position the next iteration is given by:

$$x_i = x_{i-1} + v_{i-1} \quad (8)$$

3. Case Description

Middelgrunden wind farm, an offshore wind farm 5 km from Copenhagen, is one of the earliest offshore wind farms and presents an interesting case for the application of this methodology as site and production data are publicly available. Though this is a relatively small wind farm, made up of only twenty Bonus 2 MW turbines, it still provides an interesting test case as the evaluation function can be verified for this site and the full optimization framework can also be applied.

The data available publicly includes a high level CAPEX breakdown as well as the SCADA data from 2001-2004 which contains the wind speed, wind direction, ambient turbulence intensity, and production of the wind farm at 10 min intervals. Complementing this, data from the British Oceanographic Data Centre (BODC) and the General Bathymetric Chart of the Oceans (GEBCO) to provide bathymetric data at a 30″ resolution [48]. This combination of data provides sufficient information for the evaluation function and therefore for the full optimization methodology to be applied for this real site. The site data used for this study are described in table 2.

Table 2: Data Overview

Data	Description	Source
Wind	Turbine SCADA data from 2001-2004	[49]
Turbine	Bonus B76-2000 Power and Thrust Curves	[49]
Layout	Turbine coordinates for existing layout	[49]
Bathymetry	30″ global bathymetry	[48]
Boundary	Coordinates defining the boundary	[50]
Costs	CAPEX and OPEX cost breakdown	[51, 52]

Figure 4a shows the wind distribution at the site over the four year period and fig. 4b shows the location of the wind farm and the original turbine layout built.

4. Results

4.1. Verification of Evaluation Function

The existing layout at Middelgrunden Wind Farm is comprised of a single arc running roughly north to south as shown in fig. 4b. The full cost breakdown with a comparison to the published costs is shown in table 3 based on the data provided by Larsen et al. [51] and Middelgrundens Vindmøllelaug

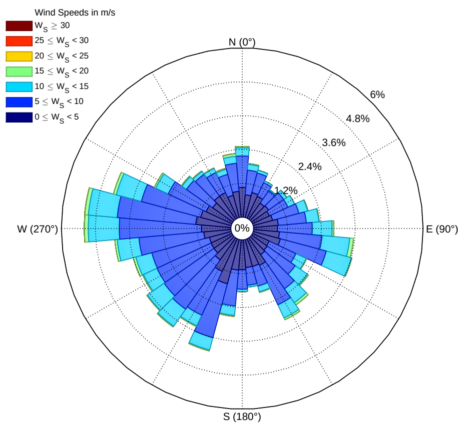

(a) Wind rose

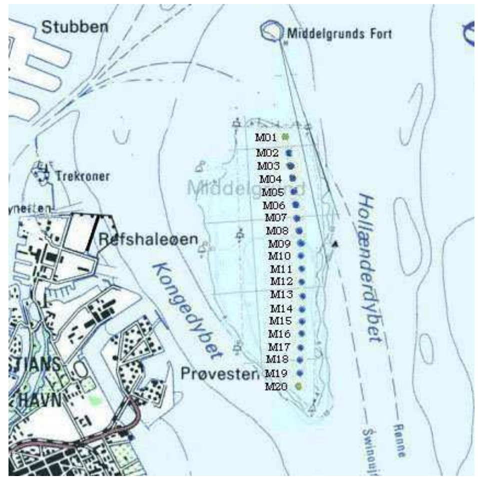

(b) Layout

Figure 4: Wind rose for 2001-2004 and existing layout at Middelgrunden Wind Farm.

I/S [52]. The costs provided by Middelgrunden wind farm have been converted to 2011-GBP as this is the currency used in the present model.

From this cost evaluation, the principal areas in which the cost estimate differs from the reported costs are the turbine costs and the O&M costs with the model over-predicting costs compared to the reported results. The reasons for this are discussed further in section 5, however, in this case, these cost differences have a minimal impact on the relative costs of the layouts during the optimization stage as the turbine supply costs are layout independent and the O&M costs only consider the average distance between the turbines and the O&M port.

Using the Larsen wake model as described and the resource data available from 2001-2004, the AEP for this period was computed for the original as-built layout and compared to the reported electricity provided to the grid over this same time period [51]. As the present model does not model or compute the availability of the wind farm, the reported 93% average availability reported over this period was used for the comparison. Table 4 shows the computed and reported AEP (including the wind farm availability) and shows that the AEP estimation for Middelgrunden is accurate with only 0.61% error over the four year period.

Combining these figures, the evaluation of the existing wind farm layout at Middelgrunden wind farm using the developed cost model therefore

Table 3: Middelgrunden - Cost Verification (£k)

	Modeled				
	CAPEX	DECEX	OPEX	Published	Error
Turbine	£35,224			£27,054	30.20%
Turbine Supply	£27,826				
Turbine Installation	£7,398				
Foundation	£13,457			£13,121	2.56%
Foundation Supply	£2,365				
Foundation Installation	£11,092				
Array Cable	£5,319			£4,573	16.30%
Array Cable Supply	£2,188				
Array Cable Installation	£3,131				
Decommissioning		£13,925			
Turbine		£7,218			
Foundation		6,707			
Project Management	£3,949				
Contingency	£9,791				
O&M			£2,424	£798	203.67%

Table 4: Middelgrunden - AEP Verification

	Computed [GWh]	Reported [GWh]	Error
AEP	95.41	96.00	-0.61%

estimates the LCOE of the wind farm to be £92.74/MWh.

4.2. Optimization of Middelgrunden Layout

During the optimization stage, 100% availability is assumed as the present methodology does not consider how the availability of the wind farm is impacted by the layout. As a result, the AEP and LCOE figures reported during the optimization are noticeably higher and lower respectively compared to the verification case considered in section 4.1.

For the given case, both the GA and the PSO were executed three times considering three different sets of constraints defined in section 2 and with the parameters given in tables 5 and 6. In the implemented GA, diversity refers to the proportion of the population that is made up of unique members and elitism to the copying of fittest individuals in the population from one generation to the next. In the PSO, the velocity must be corrected to ensure that individuals do not move beyond the search space. This is done using velocity clamping whereby the velocity is corrected to keep all individuals within the search space at all times. In the PSO, the continuous velocity must be converted for the binary implementation of the problem, and therefore a velocity transfer function is used to convert the velocity to a probability that a bit is flipped. In the present PSO, no neighborhoods were defined, and therefore only the global (gBest) neighborhood is used.

For all three constraint sets, a minimum separation constraint is applied to ensure that turbines do not risk colliding and the wind farm boundary explicitly defines the limits of the wind farm. As the three levels of placement constraint define the optimization problem differently with different decision variables and the different representations of the wind farm layout, the design spaces differ in scope. In general, the continuous mode represents the least constrained problem with the largest search space. While both the array and continuous cases make use of real encoded optimization algorithms, the binary case as it represents a series of binary decisions utilizes binary encoded optimizers.

Table 5: Genetic Algorithm Parameters

Parameter	Description
Population Size	100
Maximum Generations	1000
Probability of Crossover	Adaptive
Probability of Mutation	Adaptive
Elitism	20%
Stop Criteria	Diversity $\leq 10\%$
	$\frac{\text{Mean Score}-\text{Best Score}}{\text{Best Score}} \leq 0.001$
	Maximum generations reached
	No improvement over 50 generations

As no predefined set of allowable turbine positions was used in the development of Middelgrunden, a set of allowable turbine positions was defined for the binary optimizers. To generate this set, a triangulation was performed on the wind farm area with a target distance between vertices of 100 m. This

Table 6: Particle Swarm Parameters

Parameter	Description
Swarm Size	100
Maximum Generations	1000
Velocity Clamping	Dynamic
Velocity Transfer Function (Binary Encoding)	$T(x) = \left\lvert \frac{2}{\pi} \times arctan\left(x \cdot \frac{\pi}{2}\right) \right\rvert$
Neighborhood Topology	Global (gBest)
Stop Criteria	Diversity $\leq 10\%$
	Maximum generations reached
	No improvement over 50 generations

generated 628 allowable turbine positions within the wind farm site as shown in fig. 5.

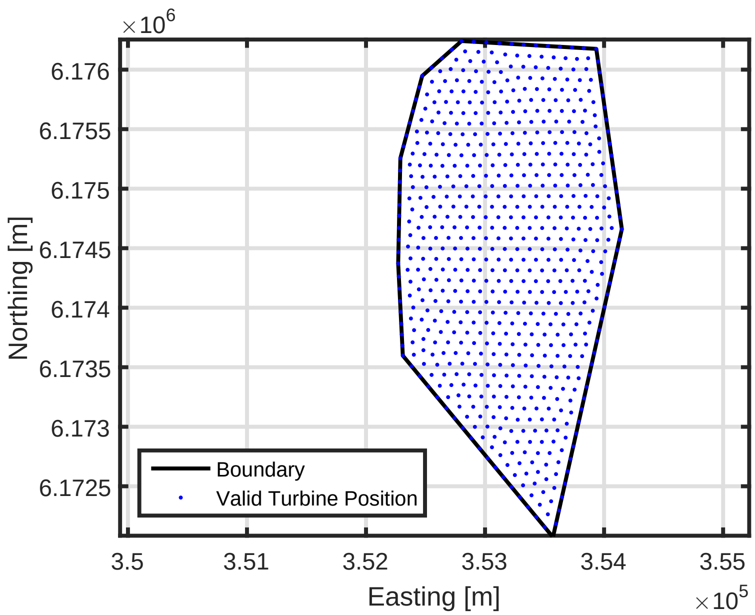

Figure 5: Allowable turbine positions for Middelgrunden Wind Farm when executing the binary decision optimizers.

Executing the two optimizers for each of the constraint sets produces the results shown in table 7 with the produced layouts plotted in fig. 6. Table 7 shows the sum of the discounted cash flow for each layout (i.e. the numerator of eq. (1)), the AEP, the computed LCOE, and the relative improvement in the LCOE compared to the as built layout evaluated using the present evaluation funciton.

Table 7: Layout Optimization of Middelgrunden Wind Farm

Case	Lifetime Cost [£]	AEP [MWh]	LCOE [£/MWh]	Improvement
Existing	9.15×10^7	1.02×10^5	86.63	-
GA - Array	9.25×10^7	1.07×10^5	83.69	3.4%
GA - Binary	9.26×10^7	1.05×10^5	85.40	1.4%
GA - Continuous	9.23×10^7	1.05×10^5	85.01	1.9%
PSO - Array	9.22×10^7	1.07×10^5	83.59	3.5%
PSO - Binary	9.24×10^7	1.05×10^5	85.13	1.7%
PSO - Continuous	9.24×10^7	1.04×10^5	85.59	1.2%

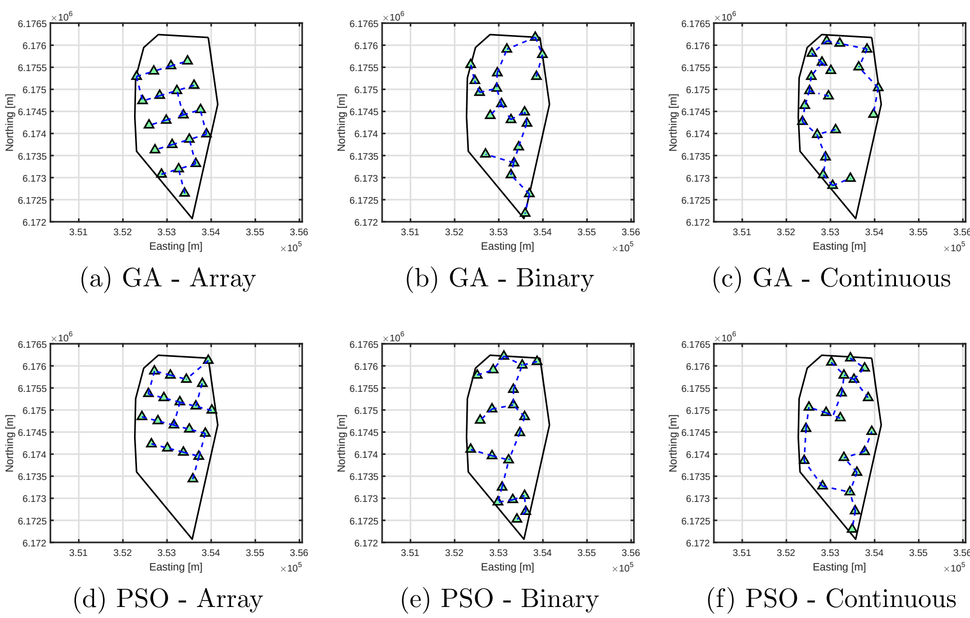

(a) GA - Array (b) GA - Binary (c) GA - Continuous

(d) PSO - Array (e) PSO - Binary (f) PSO - Continuous

Figure 6: Optimized layouts for Middelgrunden Wind Farm using both optimization algorithms and all three constraint sets.

5. Discussion

5.1. Verification of Evaluation Function

The verification results presented here showed that the AEP results for the existing layout match the reported production closely, with less than 1% error. The costs, however, had very variable error with some elements such as the foundations having low error on the order of 2.5% while others such as the turbine costs or O&M costs had over 30% and 200% error respectively.

Previous studies of Middelgrunden Wind Farm have also acknowledged that the turbine costs for this project are much lower than expected even when compared to projects using similar turbines and constructed during the same time period [4, 53, 54]. As Middelgrunden is generally thought of as an outlier when it comes to the incurred turbine costs, it is not unexpected for the turbine supply costs to carry a relatively high error.

In the case of the O&M costs, this difference can be explained by the fact that the reported figures are based on the O&M spend from two years of the project while the model estimate is the annual O&M costs anticipated through the life of the project. The modeled values therefore anticipate that some major repair works will need to be carried out during the lifetime of the project. During the two years (2003 and 2004) from which the reported costs are taken, the wind farm maintained high availability (95.9% and 95.6% respectively) indicating that no major repair works were carried out. This is further supported by qualitative reports from the wind farm [51, 52]. These two years would therefore be expected to have a lower incurred cost than the modeled values. As the wind farm is now approaching year sixteen of operation it is likely that costs more representative of the wind farm's lifetime could be available. Furthermore, the cost relationships used for the operations and maintenance term are based on reference data for wind farms of 500 MW and 1000 MW and therefore, when extrapolated to a wind farm of only 40 MW would be expected to have increased error.

Though several of the costs for Middelgrunden when estimated using this tool carry high levels of error, these cost elements are those which do not include a significant consideration of the layout (i.e. the turbine supply and O&M costs). These errors therefore will be similar for all layouts evaluated by the tool, and should not impact the optimization phase of the work.

5.2. Optimization Results

From the optimization results, it can be seen that the optimization algorithms regardless of constraint set were able to identify potential improvements with respect to the LCOE when compared to the as-built case. Interestingly, for all the cases executed, the improvement in LCOE comes as a result of an increased AEP and an increase in project cost. This indicates that for Middelgruden, the improvements in AEP outweigh the increased cost impact and it is important to consider a single metric that is impacted by both the costs and energy production in order to strike a balance between energy production and cost.

From the results of this study, it can be seen that for both optimizers and for all three constraint sets, the LCOE reductions compared to the as-built case are driven by improvements in the AEP. This suggests that for Middelgrunden, a simpler evaluation function focusing on the AEP maximization could still yield strong results, however, without the explicit consideration of the costs, the balance between energy production and project cost could result in unrealistic designs. Comparing across the three constraint sets allows an understanding of how limiting the layout to a regular grid, or a set of predefined allowable turbine positions impacts the quality in layouts. For the present site, these limitations do not significantly restrict the quality of designs that can be produced using the same optimization parameters and therefore indicates to a wind farm developer that these kind of regulatory restrictions would be acceptable. Having said that, there is scope for improving the optimizers through further parameter tuning.

As each of the constraint sets leads to different decision variables and design spaces, it would be expected that different optimization parameters such as the population size would be relevant in order to equally explore the respective search spaces. For the present study, however, the largest population size possible was used for the available computational power. Though the continuous mode was unable to reach the best results it is expected that given sufficient computational power to run the optimizers with larger population/swarm sizes would result in better results. Interestingly, at the end of each optimization run, the LCOE values had converged as would be expected, however, the individual turbine positions were also very similar between the best solutions of each run.

The relative change in discounted cost and AEP combined with information regarding the electricity sale price in each year allows the change in LCOE to be converted to an net present value (NPV). This is desirable as the TOPFARM project, Larsen et al. [55], reported *financial balance* improvements for Middelgrunden Wind Farm as a result of optimization of the wind farm layout. In the TOPFARM project, the financial balance represents the sum of the NPV improvement and further improvements as a result of reduced fatigue loading on the wind turbines through improved wake efficiencies. Though the financial balance is not directly the same as the NPV it does give a grounds for comparing against the TOPFARM results as for all cases in which the AEP increases, the financial balance improvement would exceed the NPV improvement. In a report, the TOPFARM project reported total financial balance improvements on the order of €2.1 million as a result of improvements to the layout. This would principally be realized due to reductions in the wake interactions. Using the documented electricity sale prices in each year of operation [52], the proposed layouts in the present study correspond to NPV improvements between €1.0 million and €3.5 million if considering the costs over the lifetime of the project, but revenues from only the first fifteen years. Projecting the electricity sale price for the remaining ten years of operation by assuming it remains constant at 2015 values results in a lifetime NPV improvement between €1.5 million and €4.7 million depending on which of the six proposed layouts is considered. In the TOPFARM project, the project revenues are also projected using an assumed electricity price based on the subsidy. As the equivalent financial balance improvements would be expected to be even higher as a result of the reduced wake loading, it is interesting to highlight the improvements that this work highlights when compared to TOPFARM.

The financial balance term from the TOPFARM project includes these direct increases in NPV as well as an assessment of the reduced maintenance costs as a result of reduced fatigue loading on the turbines as a result of the reduced wake interactions. As the wake efficiency of the layouts proposed by the present tool is also increased relative to the existing layout (as a result of the increased AEP) it can be expected that like the TOPFARM results further value can be assigned to the layouts as a result of the reduced fatigue loading.

Neither TOPFARM nor the present work include the visual impact constraints that the real wind farm were forced to deal with and though improvements are highlighted, these could still be unacceptable to stakeholders. By comparing the solutions provided by the tool, to the visual impact restricted layout that was built, it is possible to quantify the impacts of this constraint allowing the stakeholders to better make decisions. For future projects, quantification of constraints in this way can allow aid in developer discussions with regulators and stakeholders to ensure that the wind farm is designed as efficiently as possible given the real constraints faced for that particular site.

6. Conclusion

This paper has presented a framework for the optimization of offshore wind farm layouts and the initial result of applying it to Middelgrunden wind farm. This framework includes a more detailed approach to the estimation of the LCOE of an offshore wind farm than existing tools and is applicable to the development of future offshore wind farms. In order to establish the capabilities of this framework, the existing layout at Middelgrunden wind farm has been evaluated with less than 1% error in the estimation of the AEP when compared to published results. On the other hand, for understandable reasons, the cost estimation carried higher error, with over 200% error in OPEX and close to 20% error in the total reported CAPEX elements. This high error comes in part from the reported OPEX representing two relatively low cost operational years rather than the average over the lifetime, and Middelgrunden in general being a wind farm far below average industry costs. Even though there is relatively high error in some of the cost components, much of this error is fixed regardless of the layout under consideration and therefore the application of the optimization methodology is still relevant. Furthermore, the error led to an over-estimation of the project costs, corresponding to an erroneously high LCOE value of £92.74/MWh.

The application of two separate optimization algorithms using three different options for the constraints highlight the capabilities of this framework and also identifies potential reductions of LCOE in the range of 1-3.5% depending on which optimizer and constraints were used. This reduction in LCOE can be quite significant for a project developer, equating to an increase of NPV of up to €4.7 million. These results help illustrate the impact of potential regulatory constraints on wind farm designs. For a site such as Middelgrunden, the comparison between the layouts designed using this tool and the original as-built layout illustrate potential improvements in the layout with respect to the LCOE, but also the impact that the social constraints such as visual impact have on the LCOE.

From the results presented, both the GA and PSO produced results of similar quality indicating that the constraint set deployed has a more significant impact than which of the two optimizers is deployed. For both optimizers and each of the three constraint sets, the final population also had a series of layouts that were both similar in LCOE and turbine positions indicating that for each of the three constraint sets both optimization algorithms can find several layouts which could be of interest to the wind farm developer for further investigation.

Further development of this framework will explore validation of the evaluation function using additional wind farms, as well as the application of the framework to larger wind farms more similar to the next round of development in Europe. Given that the two optimizers never produced the same layout, there is an indication that both optimizers for all three constraint sets can be further tuned to produce further improvements in LCOE.

Acknowledgments

This work is funded in part by the Energy Technologies Institute (ETI) and RCUK energy program for IDCORE (EP/J500847/1).

References

[1] A. C. Pillai, J. Chick, L. Johanning, M. Khorasanchi, S. Barbouchi, Comparison of Offshore Wind Farm Layout Optimizaiton Using a Genetic Algorithm and a Particle Swarm Optimizer, in: Proceedings of the ASME 2016 35th International Conference on Ocean, Offshore and Arctic Engineering (OMAE 2016) Busan, South Korea, ASME, 1–11, 2016.

[2] G. Mosetti, C. Poloni, B. Diviacco, Optimization of wind turbine positioning in large wind-farms by means of a genetic algorithm, Journal of Wind Engineering and Industrial Aerodynamics 51 (1) (1994) 105–116, URL http://www.sciencedirect.com/science/article/pii/0167610594900809.

[3] S. Grady, M. Hussaini, M. Abdullah, Placement of wind turbines using genetic algorithms, Renewable Energy 30 (2) (2005) 259–270, ISSN 09601481, doi:\bibinfo{doi}{10.1016/j.renene.2004.05.007}, URL http://linkinghub.elsevier.com/retrieve/pii/S0960148104001867.

[4] C. N. Elkinton, Offshore Wind Farm Layout Optimization, Doctor of Philosophy Dissertation, University of Massachussetts Amherst, 2007.

[5] C. N. Elkinton, J. F. Manwell, J. G. McGowan, Algorithms for offshore wind farm layout optimization, Wind Engineering (2008) 67–83URL http://multi-science.metapress.com/index/Y14XL29NU6565RP1.pdf.

[6] A. Mittal, Optimization of the Layout of Large Wind Farms Using a Genetic Algorithm, Master of Science Dissertation, Case Western Reserve University, 2010.

[7] H.-S. Huang, Efficient hybrid distributed genetic algorithms for wind turbine positioning in large wind farms, IEEE International Symposium on Industrial Electronics (ISlE) (2009) 2196–2201, URL http://ieeexplore.ieee.org/xpls/abs{_}all.jsp?arnumber=5213603.

[8] T. G. Couto, B. Farias, A. C. G. C. Diniz, M. V. G. D. Morais, Optimization of Wind Farm Layout Using Genetic Algorithm, 10th World Congress on Structural and Multidisciplinary Optimization Orlando, USA (2013) 1–10.

[9] Z. W. Geem, J. Hong, Improved Formulation for the Optimization of Wind Turbine Placement in a Wind Farm, Mathematical Problems in Engineering 2013 (1) (2013) 1–5, ISSN 1024-123X, doi:\bibinfo{doi}{10.1155/2013/481364}, URL http://www.hindawi.com/journals/mpe/2013/481364/.

[10] Y. Chen, H. Li, K. Jin, Q. Song, Wind farm layout optimization using genetic algorithm with different hub height wind turbines, Energy Conversion and Management 70 (2013) 56–65, ISSN 01968904, doi:\bibinfo{doi}{10.1016/j.enconman.2013.02.007}, URL http://linkinghub.elsevier.com/retrieve/pii/S0196890413000873.

[11] P. Y. Zhang, D. A. Romero, J. C. Beck, C. H. Amon, Solving wind farm layout optimization with mixed integer programs and constraint programs, EURO Journal on Computational Optimization 2 (3) (2014) 195–219, ISSN 2192-4406, doi:\bibinfo{doi}{10.1007/s13675-014-0024-5}, URL http://link.springer.com/10.1007/s13675-014-0024-5.

[12] R. Shakoor, M. Yusri, A. Raheem, N. Rasheed, Wind farm layout optimization using area dimensions and definite point selection techniques, Renewable Energy 88 (2016) 154–163, ISSN 0960-

1481, doi:\bibinfo{doi}{10.1016/j.renene.2015.11.021}, URL http://dx.doi.org/10.1016/j.renene.2015.11.021.

[13] S. Chowdhury, J. Zhang, A. Messac, L. Castillo, Optimizing the arrangement and the selection of turbines for wind farms subject to varying wind conditions, Renewable Energy 52 (315) (2013) 273–282, ISSN 09601481, doi:\bibinfo{doi}{10.1016/j.renene.2012.10.017}, URL http://linkinghub.elsevier.com/retrieve/pii/S0960148112006544http://www.sciencedirect.com/science/article/pii/S0960148112006544.

[14] C. M. Ituarte-Villarreal, J. F. Espiritu, Optimization of wind turbine placement using a viral based optimization algorithm, Procedia Computer Science 6 (2011) 469–474, ISSN 18770509, doi:\bibinfo{doi}{10.1016/j.procs.2011.08.087}, URL http://linkinghub.elsevier.com/retrieve/pii/S1877050911005527.

[15] B. L. DuPont, J. Cagan, An Extended Pattern Search Approach to Wind Farm Layout Optimization, Journal of Mechanical Design 134 (8) (2012) 081002, ISSN 10500472, doi:\bibinfo{doi}{10.1115/1.4006997}, URL http://mechanicaldesign.asmedigitalcollection.asme.org/article.aspx?articleid=1484782.

[16] P. Fagerfjäll, Optimizing wind farm layout - more bang for the buck using mixed integer linear programming, Master of Science Dissertation, Chalmers University of Technology and Gothenburgh University, 2010.

[17] G. Marmidis, S. Lazarou, E. Pyrgioti, Optimal placement of wind turbines in a wind park using Monte Carlo simulation, Renewable Energy 33 (7) (2008) 1455–1460, ISSN 09601481, doi:\bibinfo{doi}{10.1016/j.renene.2007.09.004}, URL http://linkinghub.elsevier.com/retrieve/pii/S0960148107002807.

[18] A. Tesauro, P. Réthoré, G. Larsen, State of the art of wind farm optimization, Proceedings of EWEA 2012 (2012) 1–11URL http://proceedings.ewea.org/annual2012/allfiles2/1595{_}EWEA2012presentation.pdf.

[19] J. Herbert-Acero, O. Probst, P.-E. Réthoré, G. Larsen, K. Castillo-Villar, A Review of Methodological Approaches for the Design and Opti-

mization of Wind Farms, Energies 7 (11) (2014) 6930–7016, ISSN 1996-1073, doi:\bibinfo{doi}{10.3390/en7116930}, URL `http://www.mdpi.com/1996-1073/7/11/6930/`.

[20] NOREL Group, Nautical and Offshore Renewable Energy Liaison Group (NOREL) Minutes and Action Points from the 30th NOREL held on 17 December at DfT, Great Minister House, London SW1P 4DR (December) (2014) 1–7.

[21] A. C. Pillai, J. Chick, L. Johanning, M. Khorasanchi, V. de Laleu, Offshore wind farm electrical cable layout optimization, Engineering Optimization 47 (12) (2015) 1689–1708, ISSN 0305-215X, doi:\bibinfo{doi}{10.1080/0305215X.2014.992892}, URL `http://www.tandfonline.com/doi/abs/10.1080/0305215X.2014.992892`.

[22] Gurobi Optimization Inc., Gurobi Optimizer Reference Manual, URL `http://www.gurobi.com`, 2015.

[23] M. Lindahl, N. F. Bagger, T. Stidsen, S. F. Ahrenfeldt, I. Arana, OptiArray from DONG Energy, Proceedings of the 12th Wind Integration Workshop (International Workshop on Large-Scale Integration of Wind Power into Power Systems as well as on Transmission Networks for Offshore Wind Power Plants) London, UK .

[24] J. Bauer, J. Lysgaard, The Offshore Wind Farm Array Cable Layout Problem - A Planar Open Vehicle Routing Problem, Journal of the Operational Research Society 66 (3) (2015) 1–16, URL `http://www.ii.uib.no/{~}joanna/papers/owfacl.pdf`.

[25] S. Dutta, T. Overbye, A graph-theoretic approach for addressing trenching constraints in wind farm collector system design, 2013 IEEE Power and Energy Conference at Illinois (PECI) Urbana-Champaign, USA (2013) 48–52doi:\bibinfo{doi}{10.1109/PECI.2013.6506033}, URL `http://ieeexplore.ieee.org/lpdocs/epic03/wrapper.htm?arnumber=6506033`.

[26] R. J. Barthelmie, L. Folkerts, G. C. Larsen, S. T. Frandsen, K. Rados, S. C. Pryor, B. Lange, G. Schepers, Comparison of Wake Model Simulations with Offshore Wind Turbine Wake Profiles Measured by Sodar,

Journal of Atmospheric and Oceanic Technology 23 (7) (2006) 888–901, ISSN 0739-0572, doi:\bibinfo{doi}{10.1175/JTECH1886.1}, URL http://journals.ametsoc.org/doi/abs/10.1175/JTECH1886.1.

[27] R. J. Barthelmie, K. Hansen, S. T. Frandsen, O. Rathmann, J. G. Schepers, W. Schlez, J. Phillips, K. Rados, A. Zervos, E. S. Politis, P. K. Chaviaropoulos, Modelling and measuring flow and wind turbine wakes in large wind farms offshore, Wind Energy 12 (5) (2009) 431–444, ISSN 10954244, doi:\bibinfo{doi}{10.1002/we.348}, URL http://doi.wiley.com/10.1002/we.348.

[28] D. J. Renkema, Validation of wind turbine wake models, Master of Science Dissertation, TU Delft, 2007.

[29] A. Makridis, J. Chick, Journal of Wind Engineering Validation of a CFD model of wind turbine wakes with terrain effects, Jnl. of Wind Engineering and Industrial Aerodynamics 123 (2013) 12–29, ISSN 0167-6105, doi:\bibinfo{doi}{10.1016/j.jweia.2013.08.009}, URL http://dx.doi.org/10.1016/j.jweia.2013.08.009.

[30] G. C. Larsen, A Simple Wake Calculation Procedure, Tech. Rep., Risø National Laboratory, 1988.

[31] A. C. Pillai, J. Chick, V. de Laleu, Modelling Wind Turbine Wakes at Middelgrunden Wind Farm, in: Proceedings of European Wind Energy Conference & Exhibition 2014 Barcelona, Spain, EWEA, 1–10, 2014.

[32] M. Gaumond, P. Rethore, A. Bechmann, Benchmarking of Wind Turbine Wake Models in Large Offshore Windfarms, Proceedings of the Science of Making Torque from Wind Conference Oldenburg, Germany URL http://www.eera-dtoc.eu/wp-content/uploads/files/Gaumond-et-al-Benchmarking-of-wind-turbine-wake-models-in-large-offshore-wind pdf.

[33] DNV GL - Energy, WindFarmer Theory Manual, GL Garrad Hassan, URL https://www.dnvgl.com/services/windfarmer-3766, 2014.

[34] DNV GL - Energy, WindFarmer Validation Report, GL Garrad Hassan, URL https://www.dnvgl.com/services/windfarmer-3766, 2014.

[35] IEC, IEC 60228: Conductors of insulated cables, International Electrotechnical Commission, Geneva, Switzerland, third edn., 2006.

[36] A. Gustafsson, J. Karlstrand, G. Clasen, R. Donaghy, R. Gruntjes, A. Jensen, S. Krüger Olsen, G. Miramonti, T. Nakajima, H. Orton, J. Prieto, C. Rémy, Technical Brochure 490: Recommendations for Testing of Long AC Submarine Cables with Extruded Insulation for System Voltage above 30 (36) to 500 (550) kV, Tech. Rep., CIGRE, 2012.

[37] IEC, IEC 60287: Electric Cables - Calculation of the current rating - Part 1-1: Current rating equations (100% load factor) and calculation of losses - General, International Electrotechnical Commission, Geneva, Switzerland, second edn., 2006.

[38] G. C. Larsen, A simple stationary semi-analytical wake model, Tech. Rep. August, Risø National Laboratory, 2009.

[39] W. Tong, S. Chowdhury, J. Zhang, A. Messac, Impact of Different Wake Models On the Estimation of Wind Farm Power Generation, Proceedings of AIAA Aviation Technology, Integration, and Operations (ATIO) Indianapolis, USA 14, URL `http://arc.aiaa.org/doi/pdf/10.2514/6.2012-5430`.

[40] M. J. Kaiser, B. F. Snyder, Offshore Wind Energy Cost Modeling, Green Energy and Technology, Springer London, London, ISBN 978-1-4471-2487-0, doi:\bibinfo{doi}{10.1007/978-1-4471-2488-7}, 2012.

[41] M. J. Kaiser, B. F. Snyder, Modeling offshore wind installation costs on the U.S. Outer Continental Shelf, Renewable Energy 50 (2013) 676–691, ISSN 09601481, doi:\bibinfo{doi}{10.1016/j.renene.2012.07.042}.

[42] Bloomberg New Energy Finance, Offshore Wind: Foundations for Growth, Tech. Rep., Rabobank International, 2011.

[43] S. von Waldow, M. Wilshire, J. Wu, F. Johnston, Offshore Wind Supply Chain: Diving Into Deep Sea Foundations, Tech. Rep., Bloomberg New Energy Finance, 2013.

[44] J. H. Holland, Adaptation In Natural And Artificial Systems. [Electronic Resource] : An Introductory Analysis With Applications To Biology,

Control, And Artificial Intelligence, MIT Press, Cambridge, Mass., second edn., ISBN 0262082136, 1992.

[45] R. L. Haupt, S. E. Haupt, Practical Genetic Algorithms, Wiley-Interscience Publication, second edn., ISBN 9786468600, 2004.

[46] M. Srinivas, L. M. Patnaik, Adaptive probabilities of crossover and mutation in genetic algorithms, IEEE Transactions on Systems, Man, and Cybernetics 24 (4) (1994) 656–667, ISSN 00189472, doi:\bibinfo{doi}{10.1109/21.286385}.

[47] A. C. Pillai, J. Chick, L. Johanning, M. Khorasanchi, S. Pelissier, Optimisation of Offshore Wind Farms Using a Genetic Algorithm, in: Proceedings of the Twenty-fifth (2015) International Ocean and Polar Engineering Conference Kona, USA, ISBN 9781880653890, ISSN 1098-6189, 644–652, 2015.

[48] General Bathymetric Chart of the Oceans, The GEBCO_2014 Grid, version 20150318, URL `http://www.gebco.net`, 2015.

[49] R. Barthelmie, S. Pryor, An overview of data for wake model evaluation in the Virtual Wakes Laboratory, Applied Energy 104 (2013) 834–844, ISSN 03062619, doi:\bibinfo{doi}{10.1016/j.apenergy.2012.12.013}, URL `http://linkinghub.elsevier.com/retrieve/pii/S0306261912008951`.

[50] P.-E. Réthoré, P. Fuglsang, T. J. Larsen, T. Buhl, G. C. Larsen, TOPFARM wind farm optimization tool, Riso DTU National Laboratory for Sustainable Energy, ISBN 9788755038844, 2011.

[51] J. H. M. Larsen, H. C. Soerensen, E. Christiansen, S. Naef, P. Vølund, Experiences from Middelgrunden 40 MW Offshore Wind Farm, Proceedings of Offshore Wind Conference & Exhibition Copenhagen 2005 .

[52] Middelgrundens Vindmøllelaug I/S, Middelgrundens Vindmøllelaug Regnskab og budget, Tech. Rep., Middelgrundens Vindmøllelaug I/S, URL `http://middelgrunden.dk/?q=node/65`, 2016.

[53] S. Lundberg, Performance comparison of wind park configurations, Tech. Rep., Chalmers University of Technology, 2003.

[54] S. Krohn, S. Awerbuch, P. E. Morthorst, The economics of wind energy, Tech. Rep., European Wind Energy, doi:\bibinfo{doi}{10.1016/j.rser.2008.09.004}, URL http://www.sciencedirect.com/science/article/pii/S1364032108001299, 2009.

[55] G. C. Larsen, H. A. Madsen, N. Troldborg, T. J. Larsen, P.-E. Réthoré, P. Fuglsang, S. Ott, J. Mann, T. Buhl, M. Nielsen, H. Markou, J. N. Sørensen, K. S. Hansen, R. Mikkelsen, V. Okulov, W. Z. Shen, M. Heath, J. King, G. McCann, W. Schlez, I. Carlén, H. Ganander, E. Migoya, A. Crespo, A. Jiménez, J. Prieto, A. Stidworthy, D. Carruthers, J. Hunt, S. Gray, D. Veldkamp, A. S. Mouritzen, L. Jensen, T. Krogh, B. Schmidt, K. Argyriadis, P. Frohnböse, TOPFARM - Next Generation Desgin Tool for Optimisation of Wind Farm Topology and Operation, Tech. Rep. February, Risø DTU, Roskilde, Denmark, 2011.